

# Subunit Exchange and the Role of Dimer Flexibility in DNA Binding by the Fis Protein<sup>†</sup>

Stacy K. Merickel,<sup>‡</sup> Erin R. Sanders,<sup>‡</sup> José Luis Vázquez-Ibar,<sup>§</sup> and Reid C. Johnson<sup>\*,‡,||</sup>

Department of Biological Chemistry, School of Medicine, Howard Hughes Medical Institute, and Molecular Biology Institute, University of California, Los Angeles, Los Angeles, California 90095

Received January 9, 2002; Revised Manuscript Received March 15, 2002

**ABSTRACT:** Fis is an abundant bacterial DNA binding protein that functions in many different reactions. We show here that Fis subunits rapidly exchange between dimers in solution by disulfide cross-linking mixtures of Fis mutants with different electrophoretic mobilities and by monitoring energy transfer between fluorescently labeled Fis subunits upon heterodimer formation. The effects of detergents and salt concentrations on subunit exchange imply that the dimer is predominantly stabilized by hydrophobic forces, consistent with the X-ray crystal structures. Specific and nonspecific DNA strongly inhibit Fis subunit exchange. In all crystal forms of Fis, the separation between the DNA recognition helices within the Fis dimer is too short to insert into adjacent major grooves on canonical B-DNA, implying that conformational changes within the Fis dimer and/or the DNA must occur upon binding. We therefore investigated the functional importance of dimer interface flexibility for Fis–DNA binding by studying the DNA binding properties of Fis mutants that were cross-linked at different positions in the dimer. Flexibility within the core dimer interface does not appear to be required for efficient DNA binding, Fis–DNA complex dissociation, or Fis-induced DNA bending. Moreover, FRET-based experiments provided no evidence for a change in the spatial relationship between the two helix–turn–helix motifs in the Fis dimer upon DNA binding. These results support a model in which the unusually short distance between DNA recognition helices on Fis is accommodated primarily through bending of the DNA.

Fis<sup>1</sup> is the most abundant nucleoid-associated protein in enteric bacteria growing under nutrient-rich conditions (1–3). Fis was originally identified by its role in the regulation of site-specific DNA inversion reactions in *Salmonella* and phage Mu (4, 5). In the inversion reactions, Fis activates the DNA recombinase when the ensemble of proteins is assembled into a topologically specific nucleoprotein complex called the invertosome (6, 7). Since its initial identification, Fis has been found to function in other cellular processes including phage  $\lambda$  site-specific recombination, transcription, DNA replication at *oriC*, and chromosome segregation/cell division (8).

Fis is a small homodimeric protein consisting of two 98 amino acid subunits (9, 10). Crystallographic studies have revealed that the Fis dimer is a compact ellipsoid with mobile  $\beta$ -hairpin arms that extend into solution from the core of the protein (Figure 1A) (11–14). These N-terminal arms contact and activate the DNA recombinase to promote DNA inversion (14–16). The remainder of the Fis dimer is

composed of four  $\alpha$ -helices (A–D). The C-terminal two  $\alpha$ -helices (C and D) form the helix–turn–helix (HTH) DNA binding motif, while the N-terminal two  $\alpha$ -helices (A and B) make up the core dimerization region of the protein. The dimeric interface is primarily composed of hydrophobic amino acids along the A and B  $\alpha$ -helices of each Fis subunit (Figure 1B). The A, A' and B, B' helices are oriented in an antiparallel configuration with their side chains interdigitating (Figure 1A). Several hydrogen bond networks also connect residues of the two subunits within the dimeric core.

An aspect of the Fis structure that is unique among DNA binding proteins containing HTH binding motifs is the distance between the DNA recognition helices. The D helices in the Fis dimer are separated by about 10 Å less than the distance between major grooves on the same side of canonical B-DNA (Figure 1A) (11, 12). This short separation is found in four different crystal packing arrangements (14, 17). Therefore, the DNA, the Fis protein, or both must undergo a significant conformational change in order to form a Fis–DNA complex. Gel mobility shift assays of Fis–DNA complexes combined with DNA scission patterns produced by Fis–(1,10-phenanthroline)copper chemical nuclease chimeras have demonstrated bending of the DNA induced by Fis binding, leading to the model of the complex shown in Figure 1A (18, 19). However, a conformational change within the protein structure upon DNA binding has not been specifically addressed. DNA binding may require a quaternary change or destabilization of the dimer interface. Alternatively, DNA binding may involve an adjustment

<sup>†</sup> This work was supported by NIH Grant GM38509.

<sup>\*</sup> To whom correspondence should be addressed at the Department of Biological Chemistry, UCLA School of Medicine. Tel: (310) 825-7800. Fax: (310) 206-5272. E-mail: rcjohnson@mednet.ucla.edu.

<sup>‡</sup> UCLA School of Medicine.

<sup>§</sup> Howard Hughes Medical Institute, UCLA.

<sup>||</sup> Molecular Biology Institute, UCLA.

<sup>1</sup> Abbreviations: Fis, factor for inversion stimulation; OP-Cu, (1,10-phenanthroline)copper; HMK, heart muscle kinase; FM, fluorescein-5-maleimide; TMR, tetramethylrhodamine-5-maleimide; HTH, helix–turn–helix DNA binding motif; FRET, fluorescence resonance energy transfer; CMC, critical micelle concentration.

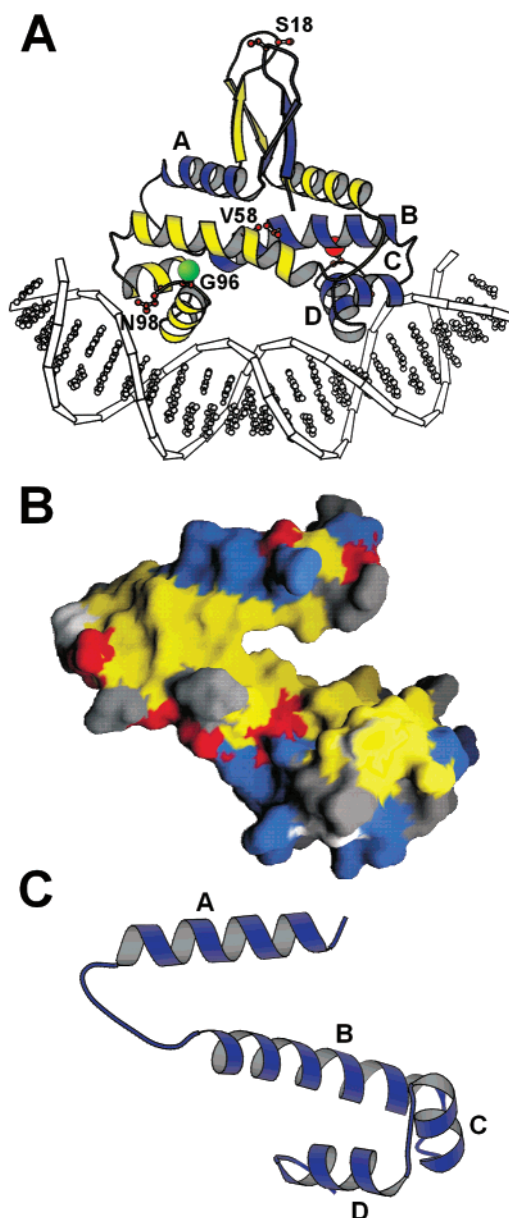


FIGURE 1: Model of the Fis dimer structure. (A) Ribbon diagram (45) of the Fis dimer structure as determined by X-ray crystallography of Fis K36E modeled onto DNA (14, 19). The Fis subunits are depicted in yellow and blue, and the DNA is schematically outlined. For both subunits the peptide chain starts at residue 10 and ends at the C-terminus (residue 98). The four  $\alpha$ -helices in the blue Fis subunit are labeled A–D. The locations of the side chains of Ser18 in the N-terminal  $\beta$ -hairpin arms, Val58 in the B helices, and Asn98 at the C-termini are shown. The green and red spheres approximate the relative positions of the FM and TMR fluorophores attached to residue 96 (not to scale). The average separation between the corresponding C $\alpha$  atoms of the seven N-terminal residues (Arg85 through Lys91) of the D and D' helices in four different crystal forms of the Fis dimer ranges from 23.0 to 25.0 Å (11, 12, 14, 17). (B) Surface representation (46) of a single subunit in the Fis dimer. Only the core of Fis, lacking the  $\beta$ -arms, is shown. Hydrophobic residues (Ala, Val, Leu, Ile, Phe, Pro, Met) and glycines are shown in yellow, acidic residues (Asp, Glu) are in red, basic residues (Arg, Lys, His) are in blue, and polar residues (Ser, Thr, Asn, Gln, Tyr) are depicted in gray. To aid in visualization, a ribbon diagram of a single subunit in the Fis dimer in the same orientation as in panel B is shown in (C). 1890–2000 Å<sup>2</sup> of the water-accessible surface area of each subunit is buried in the dimer in the four crystal forms.

within the  $\beta$ -turn connecting helix B to helix C of the HTH motif in each Fis subunit to increase the separation between the D and D' recognition helices.

During the course of experiments employing disulfide-linked heterodimers of Fis, we noticed that Fis subunits exchanged surprisingly rapidly between dimers in solution. In this report we investigate the parameters that influence the exchange of Fis subunits in solution, such as the effects of DNA binding and different solution conditions. The functional importance of the implied flexibility in the dimer interface for the formation and stability of a Fis–DNA complex and the degree of Fis-induced DNA bending was also examined. Finally, fluorescence resonance energy transfer (FRET) spectroscopy was used to investigate a DNA-induced conformational change in Fis structure.

## EXPERIMENTAL PROCEDURES

**Fis Mutants.** Isolation and functional properties of Fis S18C and N98C have been previously described (14, 19). A carboxy-terminal HMK tag (RRASV) was added to S18C using PCR, producing S18C/HMK. Fis V58C was created using the Kunkel method of site-directed mutagenesis (20), and Fis G96C was generated using a two-step PCR method (21). Fis mutant proteins were purified from cells containing derivatives of pET11a (Novagen), in which *fis* was expressed from the T7 promoter as described (19).

**Cysteine Cross-Linking Assay for Subunit Exchange.** Fis mutants S18C and S18C/HMK were reduced in 5 mM DTT at 37 °C for 1 min and mixed together (~100 ng each) in 20  $\mu$ L of reaction buffer [0.1 M NaCl, 10% glycerol, 20 mM HEPES (pH 7.5), and 200  $\mu$ g/mL BSA, except where otherwise noted]. The reactions were incubated at 37 °C for the times indicated and then oxidized by addition of 20  $\mu$ L of reaction buffer containing 4 mM (1,10-phenanthroline)-copper (2 mM OP-Cu final) and incubation at 37 °C for 1 min. The oxidation reactions were stopped by addition of 1  $\mu$ L of 0.5 M EDTA and 10  $\mu$ L of 5 $\times$  SDS loading dye without reducing agent and then frozen on dry ice. For subunit exchange assays in the presence of DNA, S18C and S18C/HMK were bound to a 20-fold molar excess of DNA fragment in reaction buffer containing 80 mM NaCl prior to being mixed together. Thirty-four base pair annealed oligonucleotides containing the distal *hin* enhancer Fis binding site (*hin-D*), 5'-AGCTTACTAGTGCAAATTGTGACCGCATTTTTGA-3', were used for the specific DNA, and 42 bp annealed oligonucleotides containing the binding site for the CRP protein, 5'-AACGAAATCCATGTGTGAAGTTGATCACAAATTTAAACACTG-3', were used for the nonspecific DNA. The proteins were separated on a 25 cm 15% SDS–polyacrylamide gel and visualized by immunoblotting using anti-Fis antibody and an alkaline phosphatase detection system. The western blots were quantitated using ImageQuant software after the filters were scanned (Molecular Dynamics).

**DNA Binding Assays.** The DNA binding affinity and DNA dissociation assays were performed and quantitated as previously described in Pan et al. (19), using a 100 bp fragment containing the *hin-D* Fis binding site as a probe. In the DNA dissociation assays, 18 nM Fis protein was bound to labeled 100 bp DNA fragments containing the *hin-D* Fis binding site for 10 min at room temperature. The Fis–DNA

complexes were then incubated with 1.4  $\mu$ M 34 bp annealed oligonucleotides containing the same *hin-D* site (~10000-fold excess) for various amounts of time before being loaded onto a 5% native acrylamide gel. DNA bending assays were performed by the method of Wu and Crothers (22) using pRJ1213, a derivative of pCY4 that contains the *hin-D* site (19, 23). Digestion with *EcoRI* releases a fragment with the Fis site near one end, and digestion with *EcoRV* releases a fragment with the Fis site near the center of the molecule. Two nanograms of each Fis mutant was bound to 100 ng of the digested pRJ1213 plasmid for 10 min at room temperature under standard binding conditions (except no salmon sperm competitor DNA was present), followed by the addition of 8  $\mu$ g/mL pBR322 competitor DNA and loading dye. The samples were loaded onto a prerunning 25 cm 8% acrylamide gel (60:1 bisacrylamide:acrylamide) and run for 16 h at 7 mA. The gel was stained with SYBR green (Molecular Probes), and the protein-bound and free DNA fragments were detected using a fluorimeter (Hitachi). Oxidized forms of S18C (96% disulfide linked), V58C (93% disulfide linked), and wild type (no cysteines present) used in DNA binding assays were produced by incubating a 50 ng/ $\mu$ L stock of Fis in dilution buffer containing 1 mM OP-Cu at 37 °C for 5 min, followed by addition of 25 mM EDTA to stop the oxidation reaction.

**Formation of Fis Conjugates with Fluorescein-5-maleimide (FM) and Tetramethylrhodamine-5-maleimide (TMR).** Two hundred micrograms of Fis G96C or N98C was reduced with 10 mM DTT for 15 min at 0 °C, followed by 1 min at 37 °C. DTT was removed by batch adsorption onto Bio-Rex 70 (Bio-Rad), followed by elution with 1 M NaCl, 10% glycerol, 20 mM HEPES (pH 7.0), 0.1 mM EDTA buffer. The reduced protein was then incubated overnight at 4 °C with a 10-fold molar excess of fluorescein-5-maleimide (FM) or tetramethylrhodamine-5-maleimide (TMR) (Molecular Probes) in 0.5 M NaCl, 5% glycerol, 20 mM HEPES (pH 7.0), 0.1 mM EDTA, 20% DMSO, and 10 mM CHAPS. The labeling reaction was stopped with 5 mM DTT, and free fluorophores were removed by batch chromatography as described above, except that 10 mM CHAPS was included in both wash and elution buffers. Fis concentrations were initially estimated using the Bradford assay (Pierce), and labeling efficiencies were initially determined spectroscopically as described by Molecular Probes. Protein concentrations and labeling efficiencies were later confirmed by SDS-PAGE, where the labeled Fis monomer migrated more slowly than the unlabeled monomer. Both methods indicated that the labeling efficiencies were between 30% and 60% for G96C and between 60% and 95% for N98C samples. Background labeling of wild-type Fis lacking any cysteine substitutions was less than 7%.

**Heterodimer Formation with N98C.** Two micrograms of Fis N98C-FM was incubated for 10 min at room temperature (23 °C) with or without DNA in 50–70  $\mu$ L of buffer A [0.1 M NaCl, 10% glycerol, 20 mM HEPES (pH 7.5)]. For reactions containing DNA, an equimolar amount of 34 bp gel-purified, annealed oligonucleotides containing the *hin-D* Fis site was added. The samples were then diluted with buffer A to a final volume of 2.5 mL and allowed to equilibrate in a 4 mL quartz fluorescence cuvette for several minutes at 37 °C with slow stirring. Two micrograms of Fis N98C-TMR was then added, and emission spectra were collected

from 510 to 650 nm immediately before and after addition of N98C-TMR at 1 min intervals using an excitation wavelength of 495 nm. To account for direct excitation of the acceptor, emission spectra obtained from mock reactions that contained only N98C-TMR were subtracted from heterodimer emission spectra. For all samples, the buffer blank was subtracted during each scan, and the spectra were corrected postscan for lamp fluctuation and wavelength variation. Fluorescence spectra were acquired using a SPEX Fluoromax-3 spectrofluorometer (Jobin-Yvon Horiba SPEX, Edison, NJ). To ensure that no absorption of donor fluorescence occurred, the OD of the samples was maintained below 0.03 (24).

**FRET with G96C Heterodimers.** One microgram of Fis G96C-FM, Fis G96C-TMR, or both was added to 50–70  $\mu$ L of buffer A plus 10 mM CHAPS. Reactions were incubated at 37 °C for 5 min to allow subunit mixing (see Figure 2D), and the samples were then diluted to 400  $\mu$ L with buffer A. Equimolar amounts of either the gel-purified 34 bp *hin-D* Fis site DNA (described above) or a 34 bp nonspecific DNA (CRP site oligonucleotide described above except 4 bp were removed from each end) were included in the plus DNA reactions, and DNA binding was allowed to occur for 10 min at room temperature (23 °C) prior to scanning. Samples were scanned in a 1 mL quartz microcell at 15 °C, and emission spectra were acquired as described above for N98C.

Because the fraction of labeled heterodimers varied with the preparation, an approach that depended on FM donor quenching was developed to assess distance changes in the absence and presence of DNA. The intensity of the FM emission maximum at ~520 nm for the G96C-FM homodimer sample in the absence ( $I_{F(-)}$ ) and presence of DNA ( $I_{F(+)}$ ) was compared using the equation:

$$(-/+ \text{ DNA})_F = I_{F(-)}/I_{F(+)} \quad (1)$$

The intensity of the FM emission maximum at ~520 nm for the heterodimer sample in the absence ( $I_{FR(-)}$ ) and presence of DNA ( $I_{FR(+)}$ ) was then compared using the equation:

$$(-/+ \text{ DNA})_{FR} = I_{FR(-)}/I_{FR(+)} \quad (2)$$

One of three scenarios could occur: (1) a  $(-/+ \text{ DNA})_{FR}$  ratio greater than the  $(-/+ \text{ DNA})_F$  ratio if, after DNA binding, there was an increase in the efficiency of energy transfer from the FM donor to the TMR acceptor due to a decrease in distance between the G96C-FM and G96C-TMR subunits, (2) a  $(-/+ \text{ DNA})_{FR}$  ratio less than the  $(-/+ \text{ DNA})_F$  ratio if, after DNA binding, there was a decrease in the efficiency of energy transfer due to an increase in distance between the G96C-FM and G96C-TMR subunits, or (3) a  $(-/+ \text{ DNA})_{FR}$  ratio equal to the  $(-/+ \text{ DNA})_F$  ratio if, after DNA binding, there was no difference in the efficiency of energy transfer, suggesting the distance between the G96C-FM and G96C-TMR subunits does not change.

## RESULTS

**Fis Subunit Exchange Measured by Cysteine Cross-Linking.** We observed rapid exchange of Fis subunits in solution after mixing dimers of distinct electrophoretic



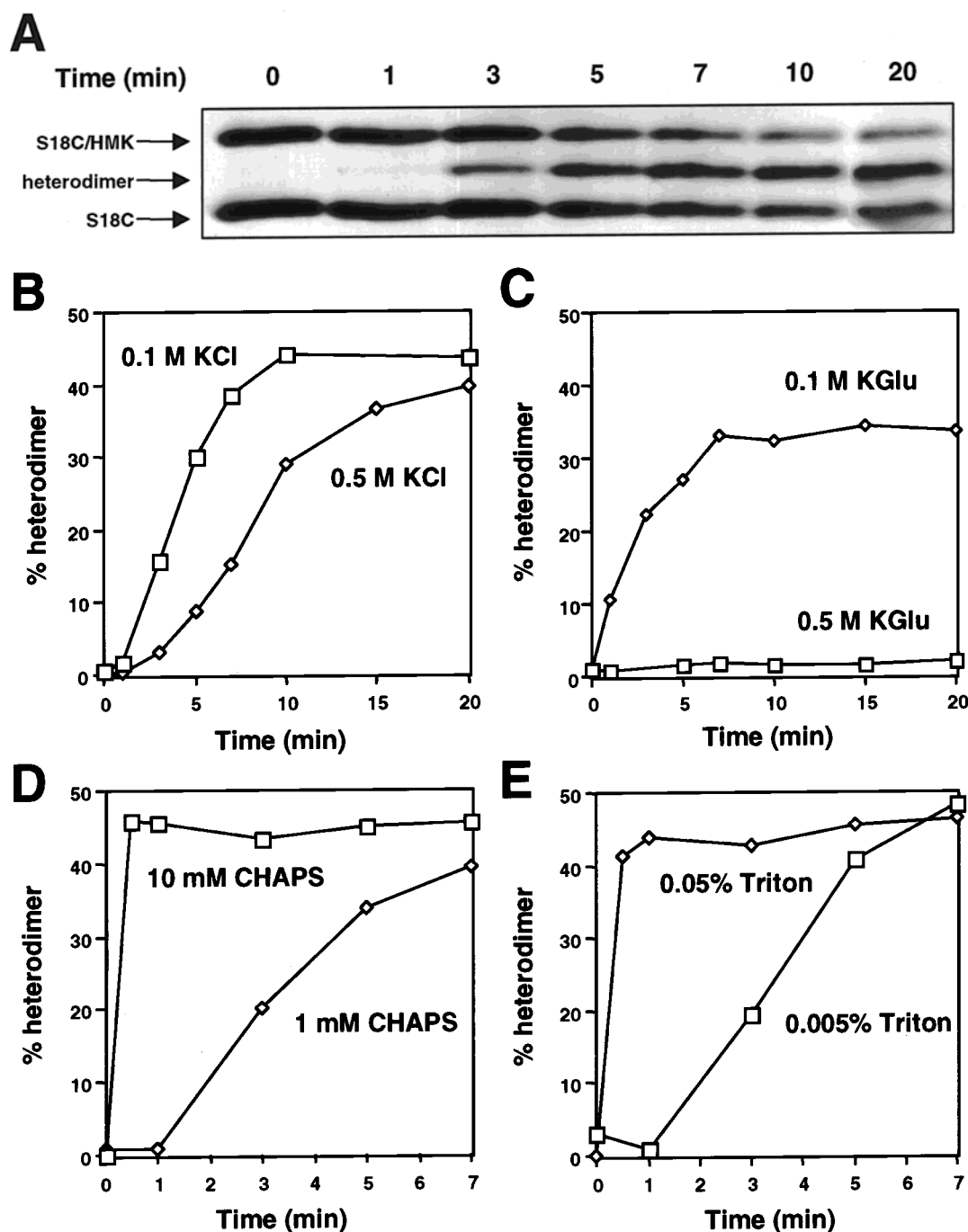


FIGURE 2: Fis subunit exchange assayed by cysteine cross-linking. Prerduced Fis S18C and S18C/HMK homodimers were mixed together and incubated at 37 °C. After different incubation times, 2 mM OP-Cu was added for 1 min to cross-link Fis dimers through a disulfide bond at Cys18. The covalently linked Fis dimers were separated by SDS-PAGE and detected by immunoblotting. (A) Representative western blot of a Fis subunit exchange experiment. The prerduced Fis S18C and S18C/HMK homodimers were mixed together and incubated for the times indicated above the lanes prior to oxidation with OP-Cu. The migrations of the covalently linked homodimers and heterodimer are designated with arrows. The heterodimer species that accumulated over time was formed by subunit exchange between the original S18C and S18C/HMK homodimers. This subunit exchange experiment was performed in standard reaction conditions containing 0.1 M KCl. (B and C) Effect of different salt concentrations on the rate of heterodimer formation. Fis subunit exchange experiments were performed in the presence of 0.1 and 0.5 M potassium chloride (B) and potassium glutamate (C). The western blots were quantitated, and the percentage of heterodimeric cross-linked Fis dimers was plotted versus time before cross-linking. (D and E) Effects of detergent concentrations above and below their CMC on the rate of heterodimer formation. Rates of heterodimer formation in the presence of 1 and 10 mM CHAPS (D) and in the presence of 0.005% and 0.05% Triton X-100 (E) are shown.

mobility. Fis mutants were employed that contained a single cysteine substitution at Ser18, which is located near the tip of the flexible N-terminal  $\beta$ -hairpin arm (Figure 1A). Previous studies have shown that Fis S18C efficiently forms disulfide-linked dimers when treated with oxidizing agents (14). Whereas oxidation of S18C rapidly covalently links

the subunits within a Fis dimer, disulfide linkage between separate Fis dimers in trans is not readily observed. The ability of S18C to cross-link dimer subunits through a disulfide bond allowed us to trap and visualize the types of dimers formed in solution. The reduced unlinked forms of Fis S18C and S18C/HMK, a Fis S18C mutant that also

contains a five amino acid heart muscle kinase (HMK) tag at the C-terminus, were mixed together and incubated at 37 °C. At various times, aliquots of the reaction were oxidized using (1,10-phenanthroline)copper (OP-Cu). Control experiments showed that 96% of the dimers were covalently linked after a 1 min incubation with OP-Cu, with most of the cross-linking occurring in the first 15 s. Electrophoresis and western blot analysis of the covalently linked dimers revealed a new band of intermediate mobility that accumulated over time (Figure 2A). This species of intermediate mobility indicates the presence of S18C:S18C/HMK heterodimers formed by subunit exchange between the original S18C and S18C/HMK homodimers. The rate of accumulation of heterodimers in a representative experiment is plotted in Figure 2B. Fifty percent of the final yield of heterodimers was obtained within about 4 min in the presence of 0.1 M KCl. No significant difference in heterodimer formation rates was observed using total Fis dimer concentrations between 0.23 and 23  $\mu$ M, suggesting a first-order reaction where dimer dissociation is limiting (data not shown).

**Exchange of Fis Subunits Measured by FRET.** Fluorescence resonance energy transfer (FRET) spectroscopy was also employed to measure the exchange of Fis subunits in solution. A Fis mutant containing a unique cysteine at its C-terminus (N98C) was conjugated with fluorescein-5-maleimide (FM) or tetramethylrhodamine-5-maleimide (TMR) to produce Fis N98C-FM or Fis N98C-TMR. The distance between residue 98 C $\beta$  atoms in four different crystal forms of wild-type and mutant Fis dimers is 37.4–38.2 Å (14, 17), which should be an appropriate distance for detecting energy transfer using the FM donor/TMR acceptor fluorophore pair (25). After an equal amount of Fis N98C-TMR was mixed with a solution of Fis N98C-FM to give a final concentration of 70 nM Fis dimers in buffer containing 0.1 M NaCl, the emission of FM at  $\sim$ 520 nm and of TMR at  $\sim$ 580 nm was monitored at 1 min time intervals. As shown in Figure 3A, after homodimer mixing there was a decrease in the FM peak together with a corresponding increase in the TMR peak as a result of energy transfer from FM to TMR due to Fis subunit exchange. The rate of heterodimer formation was estimated by quantitating the increase in N98C-TMR acceptor emission at the various time intervals (Figure 3B). By this assay, 50% of maximal exchange occurred within approximately 2 min at 37 °C.

**Factors Affecting the Rate of Subunit Exchange.** To further characterize Fis subunit exchange, we used the cysteine cross-linking assay to examine the effects of different salt and detergent concentrations as well as the presence of DNA on rates of heterodimer formation. A modest decrease in the rate of subunit exchange was observed when the concentration of KCl was increased from 0.1 to 0.5 M (Figure 2B). The rate of heterodimer formation at 0.5 M KCl was less than half that measured at 0.1 M KCl. High concentrations of potassium glutamate had a surprisingly severe inhibitory effect on subunit exchange (Figure 2C).

The presence of zwitterionic or nonionic detergents at concentrations below their CMC did not significantly alter the rate of subunit exchange (Figure 2D,E). However, increasing the detergent concentrations above their CMC, 10 mM for CHAPS and 0.05% for Triton X-100, resulted in a large increase in the rate of subunit exchange. Under these conditions, the subunits exchanged so quickly that hetero-

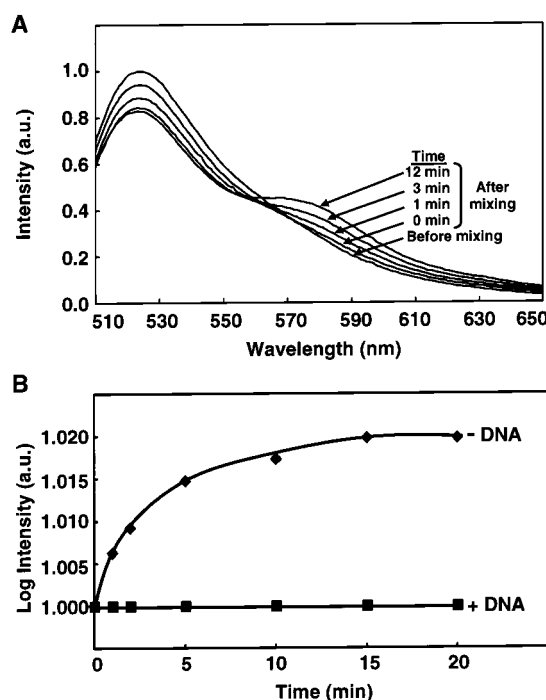


FIGURE 3: Fis heterodimer formation assayed by fluorescence resonance energy transfer (FRET). (A) Time course of normalized spectra showing heterodimer formation upon mixing of 35 nM Fis N98C-FM dimers with 35 nM Fis N98C-TMR dimers in the absence of DNA. Spectra are from a single sample that was scanned immediately before mixing and then at various times after mixing as denoted. Spectra were normalized to the maximal intensity at  $\sim$ 520 nm of the before mixing scan. (B) Rate of heterodimer formation in the absence (diamonds) and presence (squares) of DNA as quantitated from the increase in N98C-TMR acceptor emission due to energy transfer from the N98C-FM donor. For the experiment performed in the presence of DNA, Fis N98C-FM was prebound to 34 bp oligonucleotides containing a specific Fis binding site (*hin-D*). Heterodimer formation was monitored every minute for 20 min after addition of Fis N98C-TMR. To enhance visualization of the rapid change in fluorescence in the absence of DNA, the maximum intensity of the TMR peak at  $\sim$ 580 nm was plotted on a log scale. Acceptor emission was normalized by dividing the maximum intensity of the TMR emission peak at each time point after mixing by the maximum intensity of the TMR emission peak at time 0.

dimer formation was maximal within 30 s, the first time point taken. The effects of salts and detergents on the rate of heterodimer formation are consistent with the Fis dimer interface consisting of predominantly hydrophobic interactions.

The presence of DNA dramatically inhibited the exchange of Fis subunits. When S18C and S18C/HMK Fis homodimers were bound to a DNA fragment containing the *hin-D* Fis binding site prior to mixing and cysteine cross-linking, Fis heterodimers were not detectable even after the homodimers were incubated together for 60 min (Figure 4A,B). Subunit exchange in the presence of a DNA oligonucleotide containing the *hin-D* site was also assayed by FRET, and no evidence of heterodimer formation was observed over 20 min (Figure 3B). Gel mobility shift experiments demonstrated that wild-type Fis bound stably to the *hin-D* oligonucleotide with a binding constant ( $K_D$ ) of  $3 \times 10^{-9}$  M that was unaffected by the addition of excess nonspecific competitor DNA. In contrast, Fis formed dynamic complexes on nonspecific duplex DNA ( $K_D = 45 \times 10^{-9}$  M in the absence of competitor DNA), which completely exchanged onto excess unlabeled competitor DNA within 30 s of

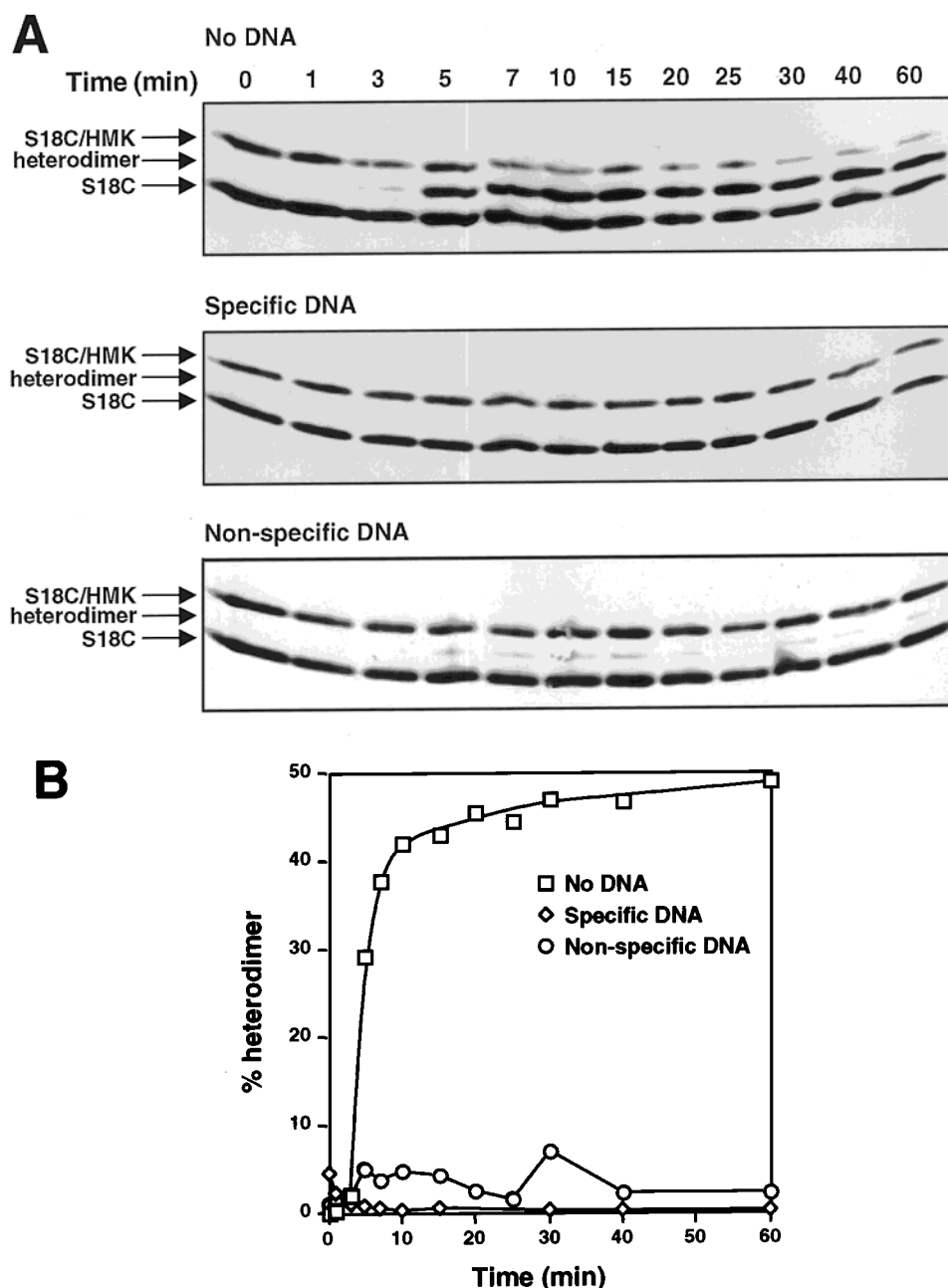


FIGURE 4: Effects of DNA binding on Fis subunit exchange. (A) Western blots of Fis subunit exchange experiments in the absence and presence of DNA. In the absence of DNA, prereduced Fis S18C and S18C/HMK homodimers were mixed together and incubated for the times indicated above the lanes prior to oxidation with OP-Cu. In the presence of DNA, prereduced Fis S18C and S18C/HMK homodimers were separately bound to either 34 bp oligonucleotides containing the *hin-D* Fis binding site or 42 bp nonspecific oligonucleotides. The prebound S18C and S18C/HMK homodimers were then mixed together and incubated for the times indicated above the lanes prior to oxidation with OP-Cu. The migrations of the covalently linked homodimers and heterodimer are designated with arrows. (B) Graphical representation of the subunit exchange data shown in (A) after quantitation. The percentage of covalently linked Fis that was in a heterodimer form was plotted versus time before cross-linking.

addition (data not shown). Nonetheless, the presence of nonspecific DNA strongly inhibited subunit exchange as measured by cysteine cross-linking (Figure 4A,B). The data suggest that both specific and nonspecific DNA binding appears to stabilize the dimeric form of Fis and greatly reduce the rate of subunit exchange.

*The Role of Fis Dimer Interface Flexibility in DNA Binding.* The ability of Fis dimers to rapidly exchange subunits in solution implies that the Fis quaternary structure is dynamic. As discussed above, the structural properties of Fis and previous biochemical characterization of Fis DNA binding raise the possibility that flexibility within the dimer

interface may be functionally important for interaction with DNA. Furthermore, previous studies have shown that the exchange of Fis dimers between DNA binding sites is strongly accelerated by DNA in trans (19). Flexibility in the dimer interface could facilitate the sequential transfer of each subunit in the dimer from one specific DNA site to another. To determine the role of dimer interface flexibility in Fis–DNA interactions, we characterized the DNA binding properties of Fis dimers in which movement within the dimer interface was restricted at different positions.

Two Fis mutants containing unique cysteine substitutions at different locations in the dimer, S18C and V58C, were

assayed for DNA binding in their reduced and oxidized forms. Oxidation of S18C covalently links the dimer subunits through a disulfide bond between the N-terminal  $\beta$ -hairpin arms of each subunit (Figure 1A). Since S18C is outside of the dimerization domain, this disulfide-linked dimer should maintain most of the flexibility in the dimer interface, although the subunits cannot completely dissociate. On the other hand, oxidation of V58C covalently links the dimer subunits through a disulfide bond between the B helices (Figure 1A). This intersubunit linkage would prevent subunit separation within the core of the dimer interface. By comparing the DNA binding properties of the oxidized disulfide-linked forms with the reduced unlinked forms of these Fis mutants, we can evaluate the role of dimer interface flexibility in DNA binding affinity, Fis–DNA complex dissociation, and DNA bending.

DNA binding isotherms of the reduced (red) and oxidized (ox) forms of S18C, V58C, and wild-type Fis are shown in Figure 5. The covalently linked oxidized forms of both S18C and V58C have slightly lower binding affinities compared to their respective unlinked reduced forms (Figure 5B,C). However, the wild-type control also exhibits a similar reduction in DNA affinity under oxidizing versus reducing conditions (Figure 5A). Since wild-type Fis does not contain cysteine residues, the small decrease in binding affinity of S18C<sup>ox</sup> and V58C<sup>ox</sup> is probably not due to the disulfide linkage between dimer subunits but rather is derived from the reversible effect of oxidizing conditions on non-cysteine residues in the protein.

We also investigated the ability of the oxidized and reduced forms of S18C, V58C, and wild-type Fis to exchange from one DNA site to another. The Fis proteins were prebound to a labeled DNA fragment containing the *hin-D* Fis binding site. The binding reactions were then incubated with an excess of unlabeled competitor DNA, which contained the same Fis binding site, and loaded onto a native gel. Exchange of the Fis mutants from the labeled DNA probe to the unlabeled competitor DNA was visualized as a decrease in binding to the labeled DNA probe over time (Figure 6). Both the oxidized and reduced forms of the S18C Fis–DNA complexes exchanged from labeled to unlabeled DNA equally well (Figure 6A). The oxidized form of V58C also exchanged from one DNA site to another as well as the reduced form (Figure 6B). Therefore, covalently linking the dimer subunits at either S18C or V58C did not inhibit the transfer of the Fis dimers between DNA sites.

The bending of DNA that accompanies Fis binding is believed to be mediated in part by the spatial relationship of the DNA recognition helices within the dimer (11, 12, 19). To examine the role of dimer interface flexibility in DNA bending induced by Fis binding, we determined the relative electrophoretic mobilities of DNA complexes formed by the oxidized and reduced forms of S18C and V58C. In these experiments, the *hin-D* Fis binding site was located either near the center or near the end of a 443 bp DNA fragment. The difference between the migrations of the Fis–DNA complexes containing the binding site near the end or center of the DNA fragment reflects the extent of DNA bending induced by Fis binding (22). As shown in Figure 7, both the reduced and oxidized forms of S18C were able to bend the DNA to the same extent as wild type. Similarly, a covalent linkage at position V58C within the Fis dimer core did not

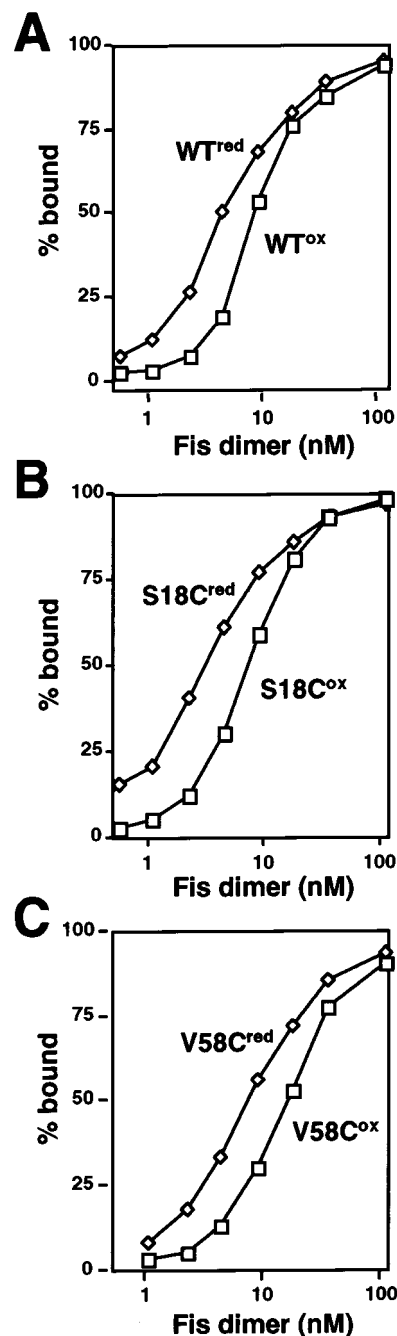


FIGURE 5: DNA binding affinities of covalently linked versus unlinked Fis dimers. Oxidized or reduced preparations of wild-type and mutant Fis proteins were incubated with a  $^{32}$ P-labeled 100 bp DNA fragment containing the *hin-D* Fis site for 10 min at 23 °C and loaded onto a native polyacrylamide gel. The percentage of DNA fragments bound in the presence of different concentrations of protein is plotted. (A) Wild-type Fis treated with OP-Cu (WT<sup>ox</sup>) or DTT (WT<sup>red</sup>). Wild-type Fis does not contain any cysteine residues. (B) Disulfide-linked (S18C<sup>ox</sup>) versus reduced (S18C<sup>red</sup>) forms of S18C. (C) Disulfide-linked (V58C<sup>ox</sup>) versus reduced (V58C<sup>red</sup>) forms of V58C.

alter DNA bending. Therefore, restricting movement within the Fis dimer core does not influence the degree of Fis-induced DNA bending.

*Changes in the Relative Positions of the Fis HTH Motifs upon DNA Binding Probed by FRET.* The C and D helices comprising the HTH motif of Fis are physically connected to the central core of the protein dimer by a potential hinge consisting of a short  $\beta$ -turn (residues 71–73) between the



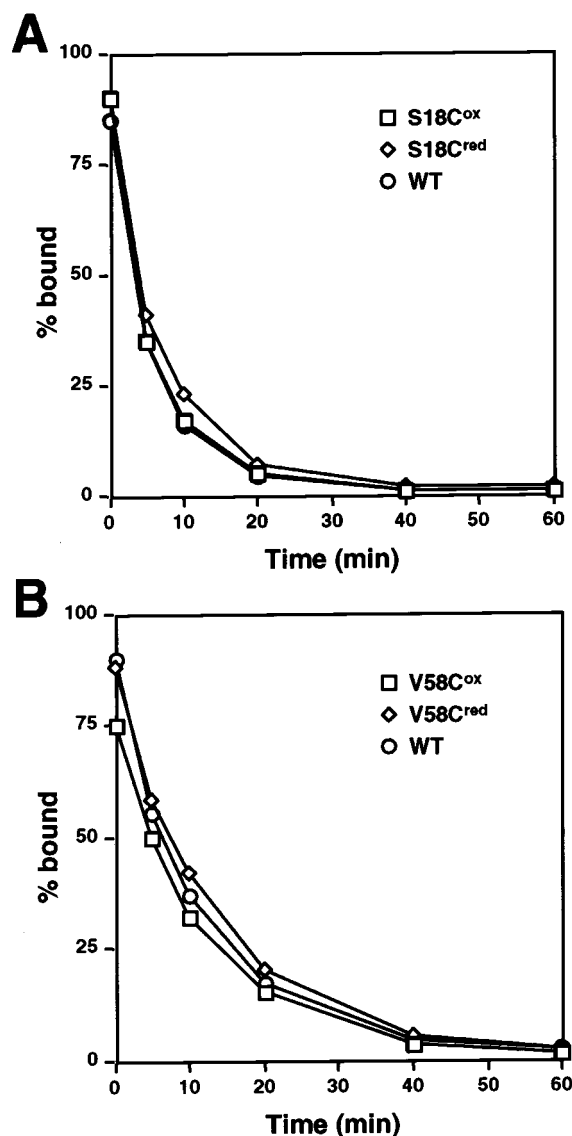


FIGURE 6: Fis–DNA complex dissociation assays on covalently linked versus unlinked Fis dimers. Oxidized or reduced preparations of Fis S18C and V58C were prebound to a labeled 100 bp DNA fragment containing the *hin-D* Fis site. An excess of unlabeled 34 bp oligonucleotides containing the same Fis binding site was added, and the binding reactions were loaded onto a native polyacrylamide gel at various times after addition of competitor. The percentage of the labeled DNA fragment bound by Fis after incubation with excess competitor DNA for the indicated times is shown. (A) Fis–DNA complex dissociation curves for S18C<sup>ox</sup>, S18C<sup>red</sup>, and WT Fis. (B) Fis–DNA complex dissociation curves for V58C<sup>ox</sup>, V58C<sup>red</sup>, and WT Fis.

B and C helices of each subunit (Figure 1A; for detailed description of the B–C  $\beta$ -turn, see ref 17). Although X-ray structures of Fis in the absence of DNA reveal networks of hydrogen bonds and van der Waals interactions that stabilize the positions of the C and D helices within the dimer, it is possible that these regions can swing out upon association with DNA. Such a movement would reposition the two recognition helices (D and D') into a more favorable location for insertion into adjacent major grooves, where the separation on one side of canonical B-DNA can range from 29 to 34 Å (12). Therefore, up to a 10 Å increase in the distance between the two D helices could be expected upon DNA binding, given that the separation observed in all crystal forms of the unbound Fis dimer is ~24 Å.

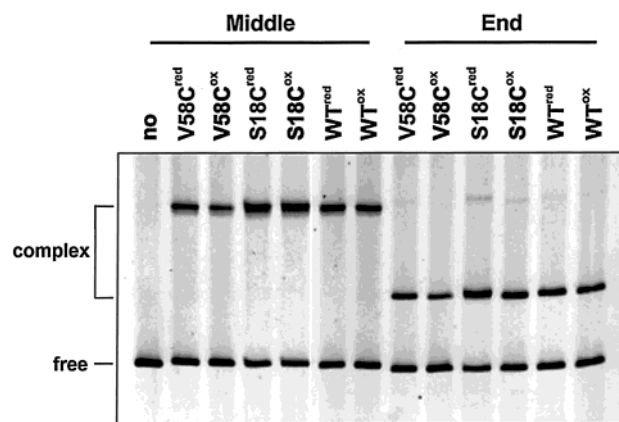


FIGURE 7: Fis-induced DNA bending by covalently linked and unlinked Fis dimers. Gel mobility shift assays were performed to determine the DNA bending properties of the oxidized and reduced forms of S18C, V58C, and WT Fis. Oxidized or reduced forms of wild-type and mutant Fis proteins were bound to a 443 bp DNA fragment containing the *hin-D* Fis binding site positioned near either the end or the middle of the fragment. The migrations of the unbound DNA fragments (free) and the DNA fragments that are bound by a Fis dimer (complex) after electrophoresis in a native polyacrylamide gel are noted. The Fis mutants used in each experiment, as well as the location of the Fis binding site on the DNA fragment, are indicated above the gel.

FRET was used to monitor a DNA-induced conformational change within the region of the Fis HTH motif. For these experiments, heterodimers of the Fis G96C mutant were formed with one subunit conjugated to fluorescein-5-maleimide (FM) and the other to tetramethylrhodamine-5-maleimide (TMR). A fluorophore coupled to residue 96 is predicted to be oriented away from the protein–DNA interface (Figure 1A), and thus its mobility would not be expected to be restricted by DNA binding. Moreover, gel mobility shift assays showed that Fis G96C-FM and G96C-TMR bound a 270 bp DNA fragment containing a specific Fis site with an affinity that was within 2-fold of wild-type Fis binding. Glycine 96 is located two residues beyond the C-terminus of helix D with a C $\alpha$  spacing of 34.6–35.4 Å as measured from four different crystal forms of wild-type and mutant Fis dimers (14, 17). Assuming an additional average separation distance of up to 10 Å due to the two fluorophores plus their associated alkyl linkers, the distance between FM and TMR coupled to Fis G96C is estimated to be about 45 Å. FRET measurements within this distance range using the FM donor/TMR acceptor pair are very sensitive since small changes in distance produce large changes in the efficiency of energy transfer (25, 26).

Emission spectra were obtained for three types of samples: the G96C-FM homodimer, the G96C-TMR homodimer, and the G96C-FM/G96C-TMR heterodimer. Each sample was prepared in triplicate and analyzed both in the absence of DNA and in the presence of either the *hin-D* Fis site or nonspecific oligonucleotides. Control experiments employing gel mobility shift assays followed by silver staining of both protein and DNA (27) showed that increasing the concentration of oligonucleotides did not increase the relative number of Fis–DNA complexes, implying that all Fis G96C was bound to DNA (data not shown).

Table 1 presents the results of four experiments from two independently labeled preparations of G96C conjugates. The G96C-FM homodimer sample produced a single emission



Table 1: Ratios of FM Donor Fluorescence Intensity in the Absence and Presence of DNA

expt <sup>a</sup>		no DNA: Fis site DNA	no DNA: nonspecific DNA
1A	(-/+ DNA) <sub>F</sub> <sup>b</sup>	1.1	1.1
	(-/+ DNA) <sub>FR</sub> <sup>c</sup>	1.0	1.0
1B	(-/+ DNA) <sub>F</sub>	1.1	1.0
	(-/+ DNA) <sub>FR</sub>	1.0	1.1
2A	(-/+ DNA) <sub>F</sub>	1.1	1.1
	(-/+ DNA) <sub>FR</sub>	1.1	1.1
2B	(-/+ DNA) <sub>F</sub>	1.1	1.1
	(-/+ DNA) <sub>FR</sub>	1.1	1.1

<sup>a</sup> Experiments reflect two independent trials (A and B) with two different labeling preparations (1 and 2) of G96C-FM and G96C-TMR. <sup>b</sup> (-/+ DNA)<sub>F</sub> represents the ratio of the average maximal intensity of the fluorescein emission peak at 520 nm for the “no DNA” homodimer sample divided by the average maximal intensity of the fluorescein emission peak for either the “plus *hln-D* Fis site DNA” or “plus nonspecific DNA” homodimer samples [ $^{av}I_{F(-)/^{av}I_{F(+)}}$ ]. <sup>c</sup> (-/+ DNA)<sub>FR</sub> represents the ratio for the heterodimer samples [ $^{av}I_{FR(-)/^{av}I_{FR(+)}}$ ] derived as described for the homodimer. The average intensities were calculated for three separately mixed but identically prepared homodimer or heterodimer samples.

peak at ~520 nm. Addition of specific or nonspecific DNA did not significantly change the G96C-FM homodimer emission peak [(-/+ DNA)<sub>F</sub> = 1.0–1.1], indicating that the presence of oligonucleotides does not alter the emission properties of fluorescein when coupled to residue 96. The G96C-FM/G96C-TMR heterodimer sample produced a fluorescein emission peak at ~520 nm and an additional sensitized tetramethylrhodamine emission peak at ~580 nm, similar to the spectra observed for the Fis N98C-FM/N98C-TMR heterodimers in Figure 3A. The fluorescein emission peak intensity from the heterodimer preparation was also not significantly different in the presence of either specific or nonspecific DNA [(-/+ DNA)<sub>FR</sub> = 1.0–1.1]. Because (-/+ DNA)<sub>FR</sub> is equal to (-/+ DNA)<sub>F</sub>, we infer that there was no difference in the efficiency of energy transfer after DNA binding, and therefore there was no change in distance between FM and TMR due to the presence of DNA. These data suggest that the HTH motif region is not repositioned upon specific or nonspecific DNA binding. Taken together with the cysteine cross-linking results reported above and the previous studies indicating DNA bending, the data support a model in which the DNA, not the protein, undergoes a conformational change upon formation of a Fis–DNA complex.

## DISCUSSION

Two independent assays revealed that Fis monomers readily exchange between dimers in solution. The first employed rapid cysteine cross-linking of subunits after mixing of homodimers of distinct electrophoretic mobilities, and the second measured energy transfer between fluorophores tethered to Fis subunits after mixing of differentially labeled homodimers. Both methods gave a dimer half-life of 2–4 min at 37 °C in 0.1 M salt. The half-life of the reaction was constant over a 100-fold range of protein concentration, consistent with a first-order reaction. The lack of dependence on Fis concentration implies that the rate-limiting step in subunit exchange is dimer dissociation.

The efficient exchange of subunits between dimers seems surprising in light of the crystal structures that show the

subunits within the dimer tightly associated in an intertwined four  $\alpha$ -helical bundle (11–14, 17). Indeed, cysteine cross-linking experiments employing <sup>32</sup>P-labeled Fis S18C/HMK suggest that the dimer–monomer transition occurs at subnanomolar concentrations (data not shown). The relative proportion of monomer to dimer after a 1 min oxidation did not increase until Fis subunit concentrations were below 0.8 nM, and equivalent amounts of subunits in the monomeric and dimeric forms were obtained at concentrations of  $\leq 0.1$  nM. We note, however, that this method may generate an artificially low value for an apparent dimerization  $K_D$  since any cross-linked dimer is prevented from dissociating into a monomer during the time frame of oxidation. Nevertheless, these results imply that Fis strongly prefers the dimeric state.

The effects of solution conditions on the rate of subunit swapping were consistent with the molecular nature of the dimer interface revealed by X-ray crystallography (11–14, 17). As shown in Figure 1B, the interface contains primarily hydrophobic amino acids, although a few hydrogen bond networks are also present which may contribute to dimer stability. Both nonionic and zwitterionic detergents dramatically increased the rate of subunit exchange when present at concentrations above their CMC. In addition, high concentrations of potassium glutamate, and to a lesser degree potassium chloride, significantly decreased the rate of subunit exchange. These properties are consistent with hydrophobic interactions being the predominant force controlling dimerization.

As noted above, DNA binding could have had a destabilizing effect on the Fis dimeric structure because of the short separation between the two HTH DNA binding motifs. However, the presence of specific or even nonspecific DNA nearly abolished subunit exchange, indicating that binding to DNA stabilizes the dimeric species.

The exchange of subunits between dimers has been previously described for other DNA binding proteins, including NtrC, CRP, Jun/Fos, C/EBP, and TF1, using a variety of detection methods (28–33). NtrC, which contains a DNA binding and dimerization domain that is homologous to Fis, displays a similar rate of heterodimer formation (28, 34). On the other hand, CRP, whose dimer interface is about 35% smaller than that of the Fis dimer, was found to exchange subunits at a much slower rate in solution (29, 33). Not surprisingly, Jun/Fos, which dimerizes through a single leucine zipper coiled-coil region, was shown to exchange at a much faster rate in solution (32). As observed with Fis, DNA binding to a specific site also inhibited subunit exchange by NtrC, CRP, Jun/Fos, and C/EBP (28–30, 32).

The dynamic nature of the Fis dimer interface that is suggested by its ability to exchange subunits led us to investigate its functional importance with respect to DNA binding, Fis–DNA complex dissociation, and DNA bending. We determined the binding properties of two cysteine mutants, S18C and V58C, in their reduced unlinked forms as well as their oxidized disulfide-linked forms. Disulfide linkage of a S18C<sup>ox</sup> dimer should maintain most of the flexibility in the dimer interface, although it cannot fully dissociate. However, covalent linkage of the V58C<sup>ox</sup> dimer will restrict movement within the dimer interface. The reduced forms of these cysteine mutants would retain any flexibility within the dimer interface. We did not observe a difference between the oxidized and reduced forms of either

S18C or V58C that was not also observed with similar treatment of wild-type Fis, which lacks cysteine, in DNA binding affinities, DNA dissociation rates, or DNA bending. Similar results have also been obtained with the Fis mutant S30C in which a disulfide bond links the A helices within the dimer (data not shown). Therefore, flexibility in the core dimer interface is not required for normal Fis–DNA interactions. Moreover, Fis dimers that are covalently linked within the dimerization core are fully functional for activating site-specific DNA inversion by Hin or activating transcription (35–37).

The DNA binding properties of disulfide-linked Fis dimers also indicate that binding is not limited by Fis dimer dissociation and are thus consistent with the subnanomolar dimerization constant estimated from the cysteine cross-linking experiment discussed above. If the Fis dimer DNA binding affinity was limited by dimer dissociation, then the covalently linked S18C<sup>ox</sup> dimer, in which complete dimer dissociation is prevented, would have a lower DNA binding affinity than the unlinked S18C<sup>red</sup> dimer. This result has been observed with  $\lambda$  repressor,  $\lambda$  Cro, and P22 Arc repressor, which all have a dimer  $K_D$  above their DNA binding affinities (38–40). In these cases, covalent linkage or tethering of the repressor subunits by an amino acid linker increases the DNA binding affinity over that observed with the unlinked dimer (39, 41, 42). In contrast to these examples, disulfide-linked and reduced forms of Fis S18C exhibit indistinguishable binding constants of  $(2\text{--}3) \times 10^{-9}$  M.

FRET-based experiments also provided evidence against a conformational adjustment within the HTH motifs of the Fis dimer upon DNA binding. One could have imagined that the recognition helices, which are separated by  $\sim 24$  Å, swing away from one another in order to more easily fit onto a DNA structure where the adjacent major grooves on one side of the helix are spaced up to 34 Å apart. Such a movement would be reminiscent of the Trp repressor dimer where the aporepressor, which cannot form a complex with DNA, has similar spacing of its recognition helices (43). The binding of tryptophan induces a conformational change that increases the spacing between recognition helices such that they can now productively interact with DNA. Fis thus far seems unique among HTH DNA binding proteins in being able to bind to DNA with such a short spacing of its recognition helices. Whereas gel electrophoresis experiments and DNA cleavage patterns by Fis–(1,10-phenanthroline)copper chimeras are consistent with an overall DNA curvature within a Fis complex of at least 50°, the details of how the DNA is distorted upon Fis binding await an atomic structure of the Fis–DNA complex (18, 19, 44).

## ACKNOWLEDGMENT

We thank Leah Corselli for isolation and purification of Fis S18C and S18C/HMK, and we thank Sarah McLeod for preparation of Fis N98C. We also thank Michael Haykinson for assisting with preparation of the figures.

## REFERENCES

- Ball, C. A., Osuna, R., Ferguson, K. C., and Johnson, R. C. (1992) *J. Bacteriol.* 174, 8043–8056.
- Osuna, R., Lienau, D., Hughes, K. T., and Johnson, R. C. (1995) *J. Bacteriol.* 177, 2021–2032.
- Talukder, A. A., Iwata, A., Nishimura, A., Ueda, S., and Ishihama, A. (1999) *J. Bacteriol.* 181, 6361–6370.
- Johnson, R. C., Bruist, M. F., and Simon, M. I. (1986) *Cell* 46, 531–539.
- Koch, C., and Kahmann, R. (1986) *J. Biol. Chem.* 261, 15673–15678.
- Johnson, R. C. (1991) *Curr. Opin. Genet. Dev.* 1, 404–411.
- van de Putte, P., and Goosen, N. (1992) *Trends Genet.* 8, 457–462.
- Finkel, S. E., and Johnson, R. C. (1992) *Mol. Microbiol.* 6, 3257–3265.
- Johnson, R. C., Ball, C. A., Pfeffer, D., and Simon, M. I. (1988) *Proc. Natl. Acad. Sci. U.S.A.* 85, 3484–3488.
- Koch, C., Vandekerckhove, J., and Kahmann, R. (1988) *Proc. Natl. Acad. Sci. U.S.A.* 85, 4237–4241.
- Kostrewa, D., Granzin, J., Koch, C., Choe, H. W., Raghunathan, S., Wolf, W., Labahn, J., Kahmann, R., and Saenger, W. (1991) *Nature* 349, 178–180.
- Yuan, H. S., Finkel, S. E., Feng, J. A., Kaczor-Grzeskowiak, M., Johnson, R. C., and Dickerson, R. E. (1991) *Proc. Natl. Acad. Sci. U.S.A.* 88, 9558–9562.
- Kostrewa, D., Granzin, J., Stock, D., Choe, H. W., Labahn, J., and Saenger, W. (1992) *J. Mol. Biol.* 226, 209–226.
- Safo, M. K., Yang, W. Z., Corselli, L., Cramton, S. E., Yuan, H. S., and Johnson, R. C. (1997) *EMBO J.* 16, 6860–6873.
- Osuna, R., Finkel, S. E., and Johnson, R. C. (1991) *EMBO J.* 10, 1593–1603.
- Koch, C., Ninnemann, O., Fuss, H., and Kahmann, R. (1991) *Nucleic Acids Res.* 19, 5915–5922.
- Cheng, Y. S., Yang, W. Z., Johnson, R. C., and Yuan, H. S. (2000) *J. Mol. Biol.* 302, 1139–1151.
- Thompson, J. F., and Landy, A. (1988) *Nucleic Acids Res.* 16, 9687–9705.
- Pan, C. Q., Finkel, S. E., Cramton, S. E., Feng, J. A., Sigman, D. S., and Johnson, R. C. (1996) *J. Mol. Biol.* 264, 675–695.
- Kunkel, T. A., Bebenek, K., and McClary, J. (1991) *Methods Enzymol.* 204, 125–139.
- Landt, O., Grunert, H. P., and Hahn, U. (1990) *Gene* 26, 125–128.
- Wu, H. M., and Crothers, D. M. (1984) *Nature* 308, 509–513.
- Prentki, P., Pham, M. H., and Galas, D. J. (1987) *Nucleic Acids Res.* 15, 10060.
- Selvin, P. R. (1995) *Methods Enzymol.* 246, 300–334.
- Van Der Meer, B. W., Coker, G. I., and Chen, S.-Y. S. (1991) in *Resonance Energy Transfer Theory and Data*, pp 148–156, John Wiley and Sons, New York.
- Lakowicz, J. R. (1999) in *Principles of Fluorescence Spectroscopy*, 2nd ed., pp 367–394, Kluwer Academic/Plenum Publishers, New York.
- Blum, H., Beier, H., and Gross, H. J. (1987) *Electrophoresis* 8, 93–99.
- Klose, K. E., North, A. K., Stedman, K. M., and Kustu, S. (1994) *J. Mol. Biol.* 241, 233–245.
- Brown, A. M., and Crothers, D. M. (1989) *Proc. Natl. Acad. Sci. U.S.A.* 86, 7387–7391.
- Shuman, J. D., Vinson, C. R., and McKnight, S. L. (1990) *Science* 249, 771–934.
- Andera, L., Schneider, G. J., and Geiduschek, E. P. (1994) *Biochimie* 76, 933–940.
- Patel, L. R., Curran, T., and Kerppola, T. K. (1994) *Proc. Natl. Acad. Sci. U.S.A.* 91, 7360–7364.
- Baker, C. H., Tomlinson, S. R., Garcia, A. E., and Harman, J. G. (2001) *Biochemistry* 40, 12329–12338.
- Pelton, J. G., Kustu, S., and Wemmer, D. E. (1999) *J. Mol. Biol.* 292, 1095–1110.
- Merickel, S. K., Haykinson, M. J., and Johnson, R. C. (1998) *Genes Dev.* 12, 2803–2816.
- McLeod, S. M., Xu, J., Cramton, S. E., Gaal, T., Gourse, R. L., and Johnson, R. C. (1999) *J. Mol. Biol.* 294, 333–346.
- Aiyar, S. E., McLeod, S. M., Ross, W., Hirvonen, C. A., Thomas, M. S., Johnson, R. C., and Gourse, R. L. (2002) *J. Mol. Biol.* 316, 501–516.

38. Bowie, J. U., and Sauer, R. T. (1989) *Biochemistry* 28, 7139–7143.
39. Robinson, C. R., and Sauer, R. T. (1996) *Biochemistry* 35, 109–116.
40. Jana, R., Hazbun, T. R., Mollah, A. K., and Mossing, M. C. (1997) *J. Mol. Biol.* 273, 402–416.
41. Sauer, R. T., Hehir, K., Stearman, R. S., Weiss, M. A., Jeitler-  
Nilsson, A., Suchanek, E. G., and Pabo, C. O. (1986) *Biochemistry* 25, 5992–5998.
42. Jana, R., Hazbun, T. R., Fields, J. D., and Mossing, M. C. (1998) *Biochemistry* 37, 6446–6455.
43. Sigler, P. B. (1992) in *Transcriptional Regulation* (McKnight, S. L., and Yamamoto, K. R., Eds.) pp 475–499, Cold Spring Harbor Press, Plainview, NY.
44. Perkins-Balding, D., Dias, D. P., and Glasgow, A. C. (1997) *J. Bacteriol.* 179, 4747–4753.
45. Kraulis, P. J. (1991) *J. Appl. Crystallogr.* 24, 946–950.
46. Nicholl, A., and Honig, B. J. (1991) *J. Comput. Chem.* 12, 435–445.

BI020019+